Int J Clin Exp Pathol 2016;9(11):11289-11300
www.ijcep.com /ISSN:1936-2625/IJCEP0039176

Original Article

Advanced oxidation protein products (AOPPs) accelerate bone loss in rats

Shuai Zheng[1*], Shuai Qin[1,2*], Zhao-Ming Zhong[1], Qian Wu[1], Ruo-Ting Ding[1], Cong-Rui Liao[1], Jian-Ting Chen[1]

[1]Department of Orthopedic Spinal Surgery, Nanfang Hospital, Southern Medical University, Guangzhou, Guangdong, PR China; [2]Department of Ophthalmology, The People's Hospital of Zhuhai, Zhuhai, Guangdong, PR China. [*]Equal contributors.

Received August 23, 2016; Accepted September 22, 2016; Epub November 1, 2016; Published November 15, 2016

Abstract: Purpose: Advanced oxidation protein products (AOPPs), markers of oxidative stress, can inhibit the proliferation and differentiation of rat osteoblast-like cells. Osteoporosis, a disease mainly results in bone loss, is closely related to oxidative stress. Whether AOPPs have any effect on bone loss in rats remains unclear. Therefore, the objective of our research is to investigate the effect of AOPPs on the bone loss of rats in vivo. Methods: Sprague-Dawley rats were divided into 4 groups (Control, RSA, AOPPs, AOPPs+SOD). PBS, rat serum albumin (RSA) and AOPPs were delivered daily by intraperitoneal injection with or without intragastric administration of superoxide dismutase (SOD) to the respective groups. Every 4 weeks, eight rats from each group were sacrificed and their blood, tibia and femur were harvested. The expression of osteocalcin and CTX in the serum was measured by ELISA, and the tibias were subjected to metaphyseal three-point bending and μCT analysis. Results: AOPPs unregulated the serum level of osteocalcin and CTX compared to the Control and RSA groups. The measurement results of μCT showed AOPPs had an effect on the decline of bone mass, while the three-point bending test revealed no significant differences in F_{max}, energy absorption and stiffness among the AOPPs and Control group throughout the investigation. No significant difference was found between the AOPPs and AOPPs+SOD group for any of the investigated parameters. Conclusion: This study demonstrated that AOPPs induced bone loss in rats. Therefore, we can infer AOPPs accelerate the development of osteoporosis in rats.

Keywords: Advanced oxidation protein products, μCT, tibia and femur of rats, osteoporosis, oxidative stress

Introduction

Osteoporosis is a systemic skeletal disease characterized by microarchitectural reduction of bone tissue leading to low bone mass and increased bone fragility. The occurrence of fractures attributable to osteoporosis can contribute to the disability and mortality of patients and may add to the economic burden of the disease. Although the etiology of osteoporosis is not well understood, previous studies have confirmed that oxidative stress is involved in the onset of the disease [1, 2].

Oxidative stress, a pathological condition characterized by a disturbance in the prooxidant-antioxidant balance, plays an important role in the development of many diseases [2-4]. Oxidative stress is a pivotal pathogenic factor of age-related bone loss and strength in mice, leading to, among other changes, a decrease in osteoblast number and bone formation [5]. The generation and survival of osteoclasts, osteoblasts, and osteocytes are greatly influenced by oxidative stress and reactive oxygen species (ROS), the main cause of oxidative stress [6, 7]. Epidemiological evidence in humans and recent mechanistic studies in rodents indicate that aging and the associated increase in ROS are the proximal culprits of osteoporosis [6].

ROS, the main cause of oxidative stress, mainly consist of H_2O_2, O_2^- and OH^-, which are generated as byproducts of the mitochondrial respiratory chain [8, 9]. The accumulation of these byproducts could damage proteins, lipids, nucleic acids and other cellular components [10]. Oxidized lipids in atherogenesis could attenuate Wnt3a-stimulated proliferation and osteoblast differentiation and stimulate the

apoptosis of osteoblastic cells, which may provide a mechanistic explanation for the link between atherosclerosis and osteoporosis [11]. Recent studies have indicated that proteins are more susceptible to oxidative damage than lipids, and therefore, proteins are generally considered to be the main original targets of ROS [12, 13].

Advanced oxidation protein products (AOPPs) were first discovered in the plasma of patients with dialysis [14]. AOPPs are a group of dityrosine-containing and cross-linking protein products formed during oxidative stress by the reaction of plasma albumin with chlorinated oxidants [15]. The plasma concentration of AOPPs is closely correlated with the level of dityrosine, a hallmark of oxidized proteins and pentosidine. These serve as markers of protein glycoxidation, which are tightly related to oxidative stress [16]. Oxidative damage to proteins is reflected in increased levels of AOPPs, which serve as novel biomarkers of oxidative stress [15].

In addition to serving as a marker of oxidative stress, AOPPs have also been shown to play a significant role as effector molecules in a number of biological events. AOPPs have been reported to induce mesangial cell perturbation through the PKC-dependent activation of NADPH oxidase [17], and the accumulation of AOPPs promote NADPH oxidase-dependent podocyte depletion by a p53-Bax apoptotic pathway both in vivo and in vitro [18]. Moreover, AOPPs are cable of inhibiting the differentiation of preadipocytes and activate inflammation in these cells [19].

The accumulation of advanced oxidation protein products (AOPPs) has been observed in many diseases, such as diabetes [17], atherosclerosis [20], rheumatoid arthritis [21] and chronic kidney disease [22]. Furthermore, all of these diseases, including diabetes [23], atherosclerosis [11], rheumatoid arthritis [24], and chronic kidney disease [25, 26], have a close relationship with osteoporosis. Additionally, we have also demonstrated that AOPPs can inhibit the proliferation and differentiation of rat osteoblasts, key cells during the genesis and development of osteoporosis, through the ROS-dependent NF-κB pathway [27]. Therefore, based on our preliminary studies, we postulate that the accumulation of AOPPs might play a role in the pathophysiological progress of osteoporosis. However, to our knowledge, there is no information available in the literature regarding the effect of AOPPs on the development of osteoporosis in vivo. Consequently, in this study, we investigated the effect of AOPPs on the development of osteoporosis using Sprague Dawley rats.

Material and methods

AOPPs-RSA preparation and determination

AOPPs-Rat Serum Albumin (RSA) was prepared as described earlier [14, 28] with minor modifications. Briefly, an RSA solution (20 mg/ml, St Louis, MO, USA) was exposed to 200 mmol/L of HOCl (Fluke, Buchs, Switzerland) for 30 min at room temperature and then dialyzed against PBS at 4°C for 24 h to remove free HOCl. Control incubation was performed in native RSA dissolved in phosphate buffer solution (PBS) alone. All of the preparations were passed through a Detoxi-Gel column (Thermo, Massachusetts, USA) to remove any endotoxin. An amebocyte lysate assay kit (Sigma, USA) was used to determine the level of endotoxin in AOPP-RSA, and the concentration of endotoxin was below 0.025 EU/ml. The AOPP content in the sample was determined as described previously [15]. Briefly, 200 μl of sample or chloramine-T was placed in a 96-well plate and 20 μl of acetic acid was added. A microplate reader was used to immediately measure the absorbance at 340 nm. The AOPP content in the AOPP-RSA and unmodified RSA was 40.10±2.23 μmol/g protein and 0.12±0.07 μmol/g protein, respectively.

Animals

Fifty-six female Sprague-Dawley rats (8 weeks old) were purchased from the Laboratory Animals center of Southern Medical University and raised in a 12 h light/dark cycle and given free access to food and tap water. The experimental animals were randomly assigned to four groups [Control, RSA, AOPPs, AOPPs+Superoxide Dismutase (SOD)] according to body weight with a daily injection of either PBS (50 mg/kg per day), native RSA (50 mg/kg per day), AOPPs (50 mg/kg per day) or AOPPs (50 mg/kg per day) with intragastric administration of SOD (Sigma Chemical, 100 mg/kg per day) separately until they were sacrificed [18].

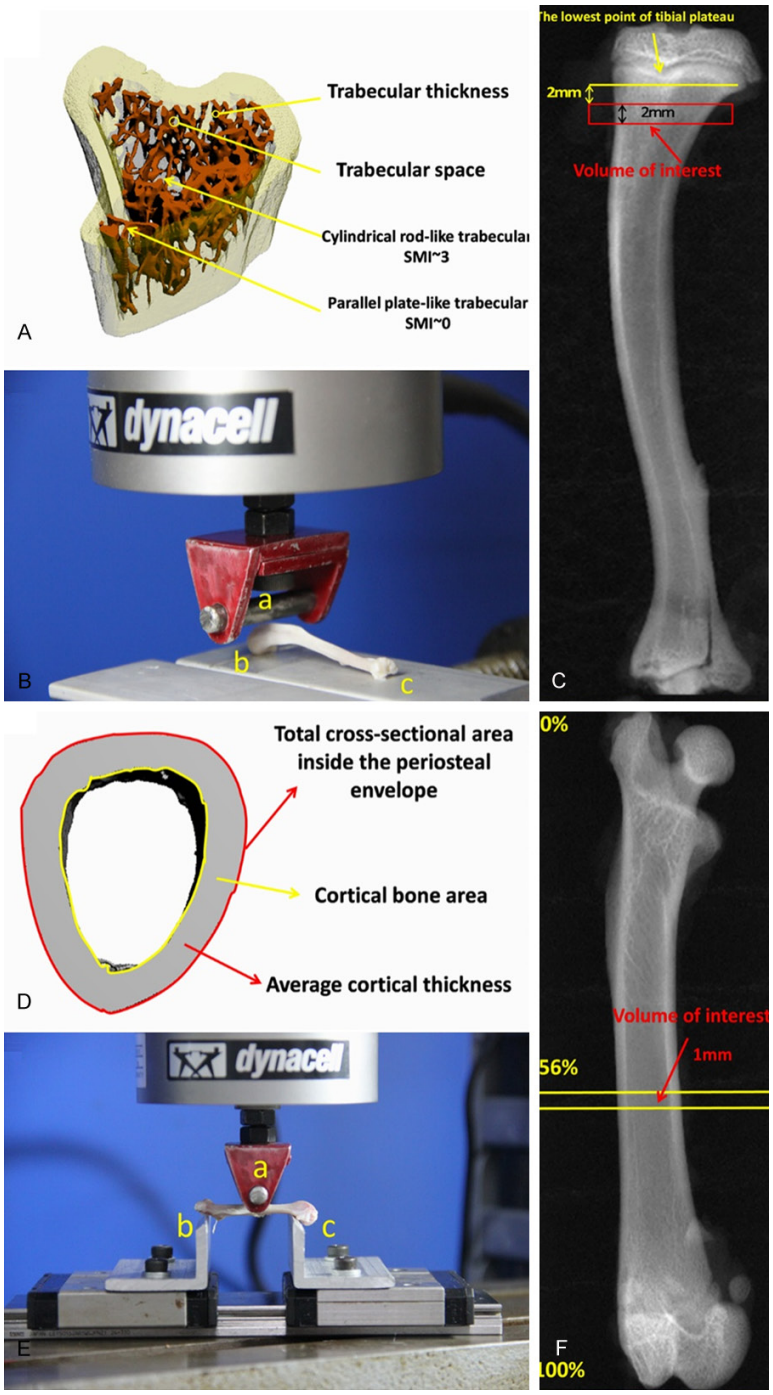

Figure 1. The general chart of the experimental methods of μCT and three-point bending test. Some of the experimental parameters of rat tibia (A) and femur (D) scanned by μCT. The design details of the three-point bending test consisting of an aluminum block and a rounded edge-free notch (B), (E). The volume of interest tested by μCT and three-point bending test (C) and (F).

The rats were sacrificed at 4 predetermined time points for the Control group (0, 4, 8 and 12 weeks) and 3 time points for the remaining three groups (4, 8 and 12 weeks). There were 32 animals in the control group and 24 animals in each of the treatment groups. The bilateral tibias and femurs were collected, with the soft tissues thoroughly removed; wrapped in normal saline soaked gauze; and stored at -20°C until use. None of the rats exhibited signs of distress or illness from the different treatments during the course of the study, and none were excluded from the study.

Serum biomarker measurements

Blood was collected from the abdominal aorta of the rats before they were sacrificed. The serum was separated by centrifugation at 4°C and stored at -80°C until required for further analysis. Osteocalcin (OC), bone formation markers, and C-terminal cross-linked telopeptides of type I collagen (CTX), which bone resorption markers, in the serum were quantified by OC and CTX ELISA kits (Cusabio, Wu Han, China), respectively, according to the protocol provided by the manufacturer. The absorbance at 450 nm was measured by a spectrophotometric plate reader.

Micro-computed tomography analysis

The micro-architecture of the trabecular and cortical bone were assessed using a high resolution micro-CT system (μCT80, Scanco Medical AG, Bassersdorf, Switzerland) equipped with a 10-μm focal spot microfocus X-ray tube as the source. Briefly, the trabecular bone architecture was analyzed at the proximal tibia, and a 2-mm region of the trabecular bone starting from 2-mm distal to the proximal growth plates (**Figure 1A** and **1C**) was

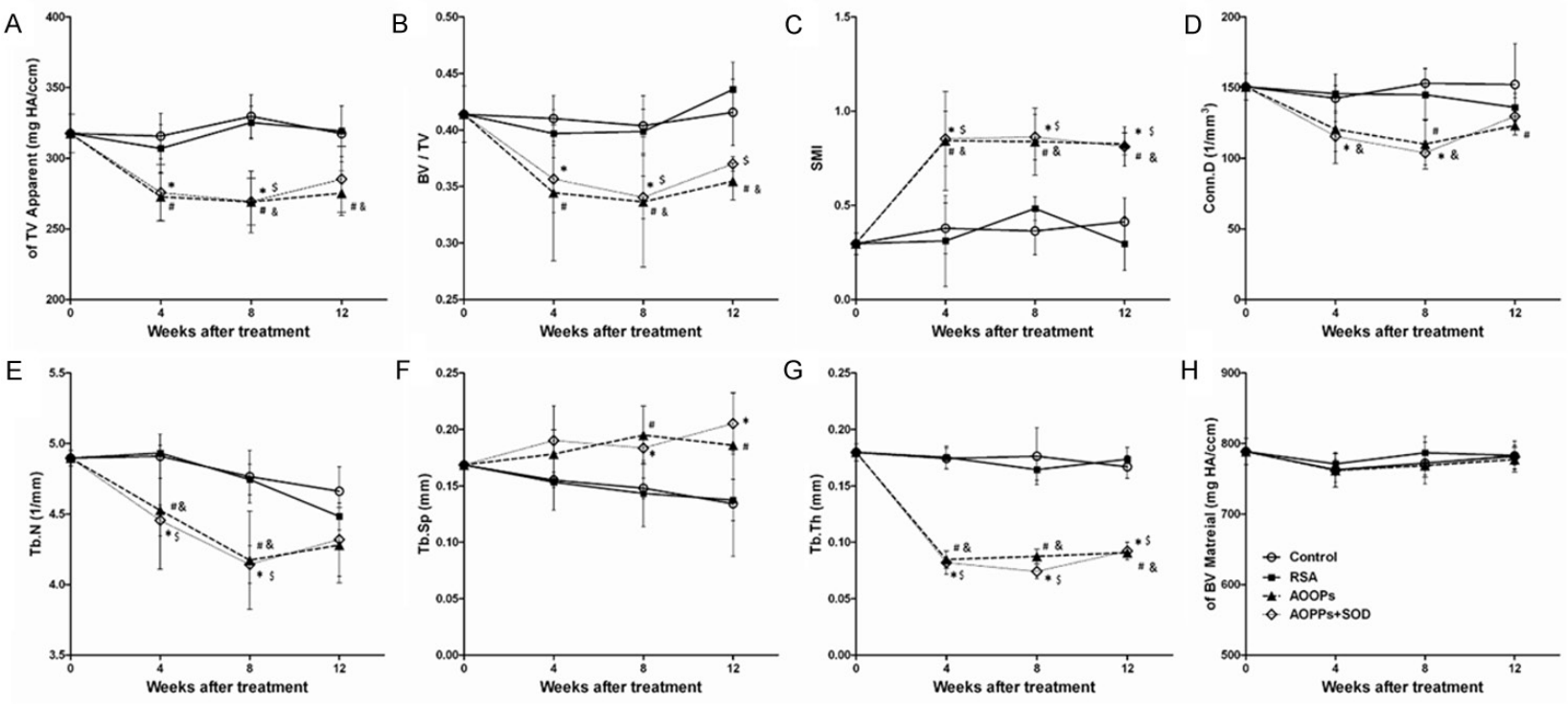

Figure 2. All of the morphological parameters (bone volume/tissue volume (BV/TV), TV apparent, BV material, structure model index (SMI), connect density (Conn.D), trabecula number (Tb.N), trabecula thickness (Tb.Th) and trabecular space (Tb.Sp)) of trabecular changes measured by μCT. The rats were randomly assigned to four groups (Control, RSA, AOPPs, AOPPs+Superoxide Dismutase (SOD)) with a daily injection of either PBS (50 mg/kg per day), native RSA (50 mg/kg per day), AOPPs (50 mg/kg per day) or AOPPs (50 mg/kg per day) with intragastric administration of SOD (100 mg/kg per day), separately. Each value was derived from a single serial cross section taken from the tibia. The X axis indicates the time in weeks after treatment. The data were presented as the mean ± SD. #: Significant difference was found between the Control group and AOPPs group ($P < 0.05$); *: Significant difference was found between the Control group and AOPPs+SOD group ($P < 0.05$); &: Significant difference was found between the RSA group and AOPPs group ($P < 0.05$); $: Significant difference was found between the RSA group and AOPPs+SOD group ($P < 0.05$).

Table 1. Change in the mechanical property at the metaphyseal tibia measured by a 3-point bending test

		Week(s) after surgery			
Groups		0	4	8	12
Osteocalcin (ng/mL)	Control	32.13±1.34	31.29±2.50	30.19±1.94	29.61±2.60
	RSA		30.15±2.05	31.89±2.02	30.96±1.01
	AOPPs		35.71±1.12[a]	35.95±1.83[b]	40.69±1.58[b]
	AOPPs+SOD		35.37±1.10	33.98±1.17[a]	41.94±0.49[b]
CTX (ng/mL)	Control	29.52±1.98	24.9±3.48	33.84±1.19	35.47±1.56
	RSA		30.01±2.87	35.94±3.46	33.64±4.10
	AOPPs		27.87±4.00	39.99±2.95[b]	46.98±3.86[b]
	AOPPs+SOD		28.56±5.60	37.88±1.96[b]	45.62±3.44[b]

Group averages are expressed as the mean ± SD. a: Significant difference from Control ($P < 0.05$); b: Significant difference from Control ($p < 0.01$).

Table 2. Quantitative analysisof bone formation (Osteocalcin) and resorption (CTX) marker levels in the serum of rats

		Week(s) after surgery			
Groups		0	4	8	12
Fmax (N)	Control	85.89±8.65	89.22±16.21	97.66±7.86	108.04±10.76
	RSA		83.55±18.38	98.80±19.98	105.10±6.96
	AOPPs		80.23±10.76	80.49±7.99[a]	111.44±5.76
	AOPPs+SOD		75.50±18.21	94.21±15.24	98.11±15.93
Energy absorption (mJ)	Control	69.89±10.61	82.69±14.81	75.38±17.62	92.48±5.76
	RSA		65.82±16.91	80.99±21.11	80.17±9.05
	AOPPs		81.12±17.24	67.93±14.96	86.54±14.70
	AOPPs+SOD		81.71±22.78	73.64±17.21	76.83±14.11
Stiffness (N/mm)	Control	121.43±10.54	119.59±11.26	132.17±20.79	139.16±7.60
	RSA		120.20±14.31	132.00±14.89	145.46±8.56
	AOPPs		115.26±14.31	123.24±10.03	145.57±19.72
	AOPPs+SOD		119.80±9.51	116.95±15.42[a]	152.31±16.73

Values are the means ± SD. a: Significant difference from Control ($P < 0.05$).

used for structural evaluation. The cortical bone architecture was analyzed at the mid-diaphyseal compartment, and a 1-mm region of the cortical bone starting at 56% of the whole femur length (calculated from the greater trochanter) was used for structural evaluation (**Figure 1D** and **1F**) according to Kohler [29]. Low-density foam was used to position the specimen tightly in the sample holder to ensure that no relative movement occurred between the specimen and the sample holder during the scan. The resultant grayscale images obtained had an isotropic voxel size of 12 μm, and the X-ray tube was operated at 55 kVp and 49 μA.

Three-point mechanical strength testing

The mechanical properties of the tibias and femurs were tested using the three-point bending method described by Sturmer [30] and performed by a miniature Instron materials testing machine (Electroplus E1000 Test System) with a 2000-N load cell (**Figure 1B** and **1E**). The tibias were thawed at room temperature for 30 min prior to testing, and the region of interest shown in **Figure 1C** and **1F** was determined using digital calipers. The samples were continuously moistened with an isotonic saline solution during the test. The speed of the feed motion was 5 mm/min with a 5% strain rate. The motion was automatically ended by a loss of strength of > 20 N or a linear change of > 2 mm. The maximum load (Fmax), energy absorption and stiffness (S) were collected via Bluehill 2 (version 2.28.832, Instron, a Division of Illinois Tool Works, Inc.). The experiment was performed blinded with regard to the association between the bones and animal groups.

Table 3. Morphologicalparameters of femur changes throughout the experiment measured by μCT and changesin the mechanical property at the midshaft femur measured by a 3-point bending test

		Week(s) after surgery			
Groups		0	4	8	12
Ct.Ar/Tt.Ar	Control	0.487±0.023	0.495±0.038	0.496±0.027	0.507±0.031
	RSA		0.464±0.184	0.479±0.020	0.514±0.026
	AOPPs		0.503±0.013	0.462±0.028	0.383±0.018[a,b]
	AOPPs+SOD		0.518±0.024	0.477±0.029	0.389±0.020[a,b]
Ct.Th (mm)	Control	0.684±0.012	0.694±0.017	0.713±0.008	0.724±0.034
	RSA		0.692±0.031	0.668±0.026	0.700±0.036
	AOPPs		0.654±0.023	0.613±0.054[a]	0.445±0.021[a,b]
	AOPPs+SOD		0.666±0.047	0.560±0.021[a,b]	0.473±0.079[a,b]
Fmax (N)	Control	161.86±13.21	157.21±19.41	162.55±21.88	157.70±10.17
	RSA		164.40±10.18	158.01±17.5	153.82±20.52
	AOPPs		153.95±6.4	144.68±21.17	137.43±7.81[a]
	AOPPs+SOD		158.79±23.38	154.65±16.17	144.00±13.52
Energy absorption (mJ)	Control	89.75±11.67	85.54±14.29	93.67±14.52	83.94±11.88
	RSA		83.95±13.01	89.53±11.87	88.94±13.04
	AOPPs		80.73±13.99	80.85±8.61	78.77±14.00
	AOPPs+SOD		84.60±11.80	85.92±14.52	76.36±16.75
Stiffness (N/mm)	Control	141.43±12.59	145.98±10.50	152.09±16.80	159.75±16.92
	RSA		139.38±15.01	160.57±19.23	155.39±17.59
	AOPPs		130.40±11.44	144.29±9.88	165.72±15.57
	AOPPs+SOD		141.16±10.57	157.74±16.12	157.05±11.85

Group averages are expressed as the mean ± SD. a: Significant difference from Control ($P < 0.05$); b: Significant difference from RSA ($P < 0.05$); Tt.Ar: Total cross-sectional area inside of the periosteal envelope; Ct.Ar: Cortical bone area; Ct.Ar/Tt.Ar: Cortical area fraction; Ct.Th: Average cortical thickness.

Statistical analysis

The results were expressed as the mean ± standard deviation. Significant differences between different groups for the same time or over the entire period were compared using one-way ANOVA. The homogeneity variance was compared among the groups first. Multiple comparisons were performed using the LSD or Dunnett's C method. The statistical significance was assumed at $P < 0.05$, and the statistical analyses were performed with SPSS 13.0 software.

Results

Micro-computed tomography (μCT)

The morphological alterations of the trabecular microarchitecture in the tibial and cortical bone in the femur measured from μCT are shown in **Figure 2** and **Table 3**. The representative three-dimensional micro-CT reconstruction images of the tibia and femur are illustrated in **Figures 3** and **4**.

From 4 to 12 weeks, all of the morphological parameters in the AOPPs and AOPPs+SOD groups showed a significant difference from the control and RSA groups (bone volume/tissue volume (BV/TV), TV apparent, structure model index (SMI), connect density (Conn.D), trabecula number (Tb.N), trabecula thickness (Tb.Th) and trabecular space (Tb.Sp)) ($P < 0.05$ or 0.01), except for the BV material. The damage effect of AOPPs on the trabecular architecture was apparent at week 4, but the effect was not aggravated at week 8 and week 12.

Compared with their respective control groups, significant changes were detected in the AOPPs group at week 4, week 8 and week 12 for almost all of the tested indices: TV apparent (-13.6%, $P = 0.006$; 18.4%, $P = 0.001$ and -13.3%, $P = 0.019$), BV/TV (-16.0%, $P = 0.016$; 16.7%, $P = 0.032$ and -14.7%, $P = 0.015$), Tb.Th (-51.4%, 50.4%, and -45.6%, $P < 0.001$ for all), SMI (+122.7%, $P = 0.043$; +130.1%, $P = 0.002$ and +99.9%, $P < 0.001$), Tb.Sp (+14.9%, $P = 0.409$; +31.8%, $P = 0.035$ and +38.6%, $P =$

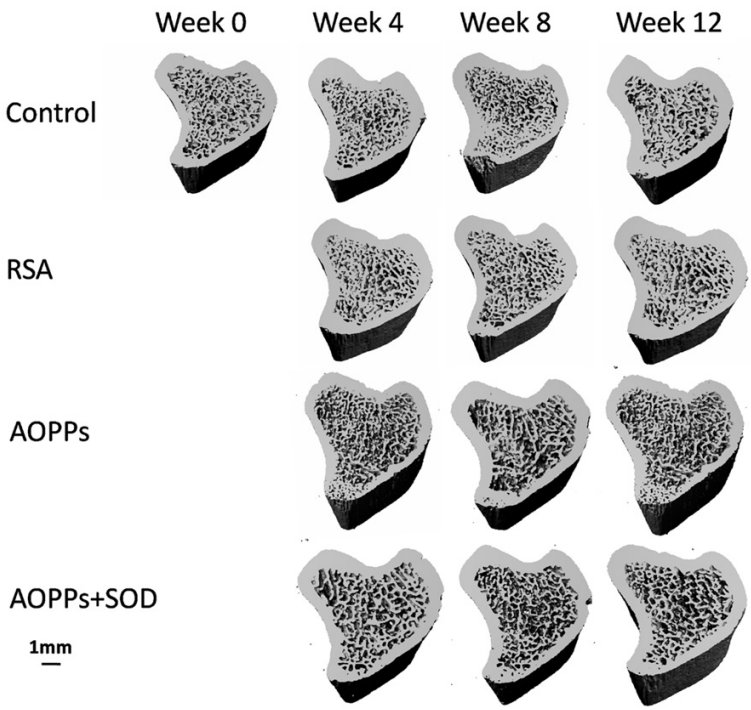

Figure 3. Three-dimensional μCT images of the tibia metaphyseal of the Control, RSA, AOPPs and AOPPs+SOD groups at the time of treatment and follow-up measurements 4, 8 and 12 weeks later. Images were chosen from the animals with median cancellous BV/TV values.

0.007), Conn.D (-15.5%, P = 0.322; -28.1%, P = 0.001 and -19.1%, P = 0.014), Conn.D (-7.8%, P = 0.008; -12.4%, P = 0.001 and -8.2%, P = 0.186), except for the BV material compared to the Control group. All of the above parameters in the RSA group exhibited no significant difference from the Control group, and the same phenomenon occurred between the AOPPs and AOPPs+SOD group.

At week 12 only, both of two morphological parameters, Cortical bone area/Total cross-sectional area inside the periosteal envelope (Ct.Ar/Tt.Ar) and Average cortical thickness (Ct.Th), in the AOPPs and AOPPs+SOD groups showed a significant difference from the control and RSA groups (P < 0.01). At week 8, the Ct.Th in the AOPPs and AOPPs+SOD groups exhibited significant differences compared with the control group (P < 0.05 or 0.01). Significant changes were also detected in the AOPPs+SOD group at week 8 compared with the RSA group for Ct.Th (P < 0.01).

Biomechanical quality of the tibia and femur

The mean maximum load (F_{max}), energy absorption and stiffness for the tibia and femur in all four groups at different time points are shown in **Tables 1** and **3**. As the rats became older, the F_{max} of the tibia in the control group increased from 85.89±8.65 N at week 0 to 108.04±10.76 N at week 12 (+25.0%), but a significant difference was found only at week 8 (P = 0.0033) between the Control and AOPPs groups. The AOPPs+SOD group exhibited significantly lower stiffness than the Control group at week 8 (P = 0.035); however, there was no significant difference between energy absorption in any of the groups throughout the study. No significant difference was found between the AOPPs and RSA group in the above three parameters. Only the F_{max} of the femur in the AOPPs group at week 12 showed a significant difference from the control group (P = 0.029).

Biochemical parameters of serum

The results for osteocalcin and the CTX levels of the different groups at different times are shown in **Table 2**. The serum osteocalcin level in the AOPPs group was significantly elevated compared to control animals at week 4 (P = 0.042), week 8 (P = 0.002) and week 12 (P < 0.001). Moreover, a significant difference was found in the AOPPs+SOD group compared to the control group at week 8 (P = 0.024) and week 12 (P < 0.001).

Regarding bone reabsorption, the AOPPs group showed a significantly higher level than the control group at week 8 (P = 0.008) and week 12 (P = 0.001). Furthermore, the AOPPs+SOD group also exhibited an elevated level of CTX at week 8 (P = 0.006) and week 12 (P = 0.001) compared with the control group. At no point in the study was a significant difference found between the RSA and AOPPs+SOD groups for both osteocalcin and CTX.

Discussion

Micro-CT, also called μCT, has become one of the most important methods to evaluate bone

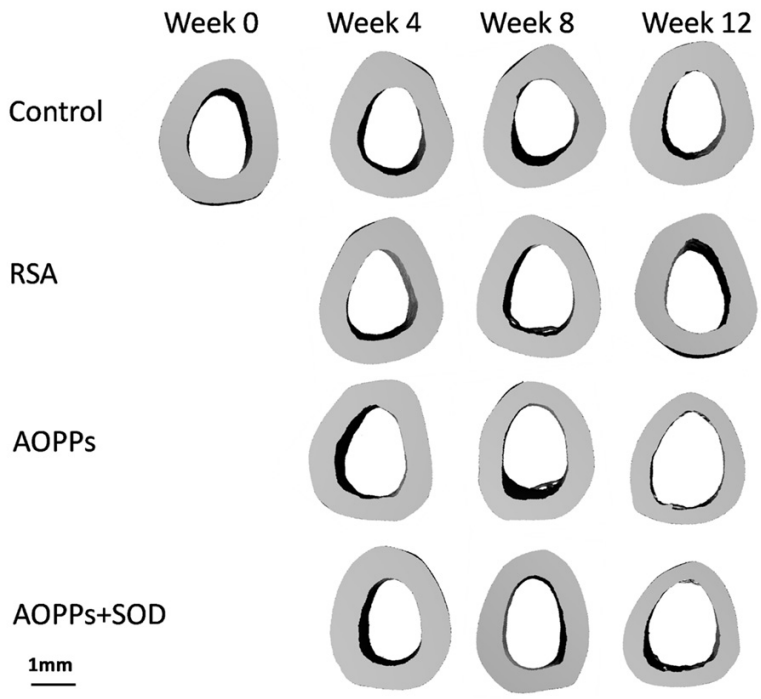

Figure 4. Three-dimensional μCT images of the femur mid-diaphyseal of the Control, RSA, AOPPs and AOPPs+SOD groups at the time of treatment and follow-up measurements 4, 8 and 12 weeks later. Images were chosen from the animals with median Ct.Ar/Tt.Ar. Tt.Ar: Total cross-sectional area inside of the periosteal envelope; Ct.Ar: Cortical bone areal; Ct.Ar/Tt.Ar: Cortical area fraction.

morphology in animal models. The accuracy of the μCT morphology measurements has been evaluated by comparison with traditional measures from 2D histomorphometry both in animal [31-33] and human specimens [34, 35]. These studies show that morphologic measurements by μCT are generally highly correlated with those from histomorphometry. Compared with histological analyses, μCT can measure the bone microarchitecture directly without relying on stereological models, and therefore, μCT has become the "gold standard" for the evaluation of bone morphology and microarchitecture in rats and other small animal models [36]. Furthermore, the assessment of bone morphology by μCT scanning is nondestructive, and thus, samples can be used subsequently for other assays, such as mechanical testing. Therefore, to perform a three-point bending test, histomorphometry was replaced by μCT to evaluate the bone morphology of the rats in our experiment.

μCT 80 was used in this study, where it provided the bone microarchitecture parameters of TV apparent and BV material in addition to the traditional parameters, such as BV/TV, Tb.Th, Tb.N, Tb.Sp, SMI and Conn.D. TV apparent is used to describe the mean density of the volume of interest, and BV material relays the mean density of the trabecular bone in the region of interest.

AOPPs, dityrosine-containing and cross-linking protein products formed during oxidative stress by the reaction of plasma albumin with chlorinated oxidants [15] were obtained by exposing the RSA solution to HOCl in this study. RSA could not be thoroughly consumed in the reaction, and some RSA might be left. Consequently, the RSA solution was injected into rats to test whether RSA had any effect on the tibia. The data presented in the RSA group showed no significant difference with the control group in almost all of the test parameters. Hence, we concluded that the AOPPs, and not RSA, affected the tibia in the rats.

In addition, the data of the tibia provided by μCT revealed that the micro-architectural bone parameters in the AOPPs group showed a significant difference from the control group in almost all of the tested indices at week 4. Therefore, we speculated that AOPPs could aggravate the bone loss of the tibia in rats; however, at week 8 and week 12 in the AOPPs group, the difference was not obvious compared with week 4. Furthermore, TV apparent, BV/TV, Conn.D and Tb.N at week 12 were higher than that of week 8, which indicated that at 12 weeks, the bone mass loss was less than at 8 weeks. On the basis of these results, AOPPs had limited effects on trabecular architecture. Furthermore, as the rats grew older, the tibia became increasingly stronger, allowing it to counteract some of the damaging effects of AOPPs on the trabeculae. Therefore, the degree of bone mass loss at week 12 was less than that of week 8. The data of the femur measured

by μCT revealed that the cortical bone was more solid than the trabeculae and was not susceptible to AOPPs. The data of the tibia showed that compared with the control group, a significant difference was found in the AOPPs group at week 4, while a significant difference was found at week 12 regarding the femur. On the basis of these results, AOPPs had continuous damaging effects on the bone of rats, and thus, AOPPs may play an important role in the development of osteoporosis.

A three-point bending test was adopted in this experiment to evaluate bone strength. At week 8, the tibia treated with AOPPs had a significantly lower F_{max} than the control group. When stiffness was studied, there was a significant difference at week 8 between the AOPPs+SOD group and control group; however, there was no significant difference in energy absorption within all four of the groups. In addition, almost no significant difference was found in the three-point bending test regarding the femur. These observations could be due to AOPPs having a limited impact on bone mass loss or because the bone strength was not weakened enough to be detected by the three-point bending test. Furthermore, a large standard deviation of the test subjects may have limited the significant differences found in the three-point bending test.

Osteocalcin, a non-collagenous protein synthesized by mature osteoblasts, is generally regarded as a specific marker of bone formation [37, 38], and CTX, a collagen degradation product released by osteoclasts, is considered as a marker of bone resorption [39, 40]. Lerner [41] reported that in postmenopausal osteoporosis, bone-resorption as well as bone-formation was increased. Osteocalcin level increases were not due to individual osteoblasts producing more osteocalcin, but rather because of the increasing number of bone-forming osteoblasts. From **Table 2** we can observe that both osteocalcin and CTX were elevated in the AOPPs-treated animals, especially in the AOPPs group. These results suggested that the AOPPs challenge activated both osteoblasts and osteoclasts in rats. Therefore, we believe that the number of active osteoblasts and osteoclasts was increased by AOPPs, which resulted in the upregulation of osteocalcin in the serum as well as CTX.

SOD is antioxidant enzymes that can convert superoxide to hydrogen peroxide and thus can prevent superoxide accumulation [42]. An increase of AOPPs and MDA and a decrease in SOD has been observed in some pathophysiologic processes, including aging [43] and postmenopausal bone loss [44]. Our previous study demonstrated that SOD could reverse the AOPPs-induced inhibition of ROB cell proliferation and differentiation in vitro [27], and consequently, we hypothesized that SOD could prevent the occurrence and development of osteoporosis induced by AOPPs. However, in contrast to our supposition, the AOPPs+SOD group did not show any significant difference compared to the AOPPs group in almost all of the experimental results. The effect of AOPPs could be reversed by SOD in vitro, but did not produce the same result in vivo. In addition, some studies reported that SOD also played an important role in bone resorption. Frasr et al [45] reported that the combination of xanthine and xanthine oxidase, which generates superoxide anions, failed to stimulate bone resorption, except in the presence of SOD, which resulted in a modest increase in bone resorption. Furthermore, Suda et al. [46] found that SOD enhanced the formation of osteoclast-like cells, implying that the generation of H_2O_2 by SOD from endogenously produced superoxide may play a role in osteoclast formation. Therefore, the exact mechanism of SOD's effect on AOPPs in vivo requires more investigations.

Conclusion

This study demonstrated that AOPPs increase bone loss in rats and that the progress could not be altered by the antioxidant enzyme, SOD. These results suggest that the serum level of AOPPs might accelerate the development of osteoporosis, which may provide new targets for intervention.

Acknowledgements

This work was supported in part by the National Natural Science Foundation of China (No. 816-01944 and No. 81272042), Guangdong Natural Science Foundation (No. 2015A030310481), Guangdong Science and Technology Program key projects (N0. 2016A020215100 and No. 2013B021800144).

Disclosure of conflict of interest

None.

Address correspondence to: Shuai Zheng and Jian-Ting Chen, Department of Spinal Surgery, Nanfang Hospital, Southern Medical University, 1838 North Guangzhou Avenue, Guangzhou, PR China. Tel: +86-20-61641723; Fax: +86-20-61641721; E-mail: zhengshuai041@qq.com (SZ); chenjt99@tom.com (JTC)

References

[1] Valli A, Suliman ME, Meert N, Vanholder R, Lindholm B, Stenvinkel P, Watanabe M, Barany P, Alvestrand A, Anderstam B. Overestimation of advanced oxidation protein products in uremic plasma due to presence of triglycerides and other endogenous factors. Clin Chim Acta 2007; 379: 87-94.

[2] Garrett IR, Boyce BF, Oreffo RO, Bonewald L, Poser J, Mundy GR. Oxygen-derived free radicals stimulate osteoclastic bone resorption in rodent bone in vitro and in vivo. J Clin Invest 1990; 85: 632-639.

[3] Stanojkovic I, Kotur-Stevuljevic J, Milenkovic B, Spasic S, Vujic T, Stefanovic A, Llic A, Ivanisevic J. Pulmonary function, oxidative stress and inflammatory markers in severe COPD exacerbation. Respir Med 2011; 105 Suppl 1: S31-S37.

[4] Zhang Y, Zhong Z, Hou G, Jiang H, Chen J. Involvement of Oxidative Stress in Age-Related Bone Loss. J Surg Res 2011; 169: e37-e42.

[5] Almeida M, Han L, Martin-Millan M, O'Brien CA, Manolagas SC. Oxidative stress antagonizes Wnt signaling in osteoblast precursors by diverting beta-catenin from T cell factor- to forkhead box O-mediated transcription. J Biol Chem 2007; 282: 27298-27305.

[6] Manolagas SC. From estrogen-centric to aging and oxidative stress: a revised perspective of the pathogenesis of osteoporosis. Endocr Rev 2010; 31: 266-300.

[7] Manolagas SC, Parfitt AM. What old means to bone. Trends Endocrinol Metab 2010; 21: 369-374.

[8] Cabiscol E, Piulats E, Echave P, Herrero E, Ros J. Oxidative stress promotes specific protein damage in Saccharomyces cerevisiae. J Biol Chem 2000; 275: 27393-27398.

[9] Karihtala P, Soini Y. Reactive oxygen species and antioxidant mechanisms in human tissues and their relation to malignancies. APMIS 2007; 115: 81-103.

[10] Valentine JS, Wertz DL, Lyons TJ, Liou LL, Goto JJ, Gralla EB. The dark side of dioxygen biochemistry. Curr Opin Chem Biol 1998; 2: 253-262.

[11] Almeida M, Ambrogini E, Han L, Manolagas SC, Jilka RL. Increased lipid oxidation causes oxidative stress, increased peroxisome proliferator-activated receptor-gamma expression, and diminished pro-osteogenic Wnt signaling in the skeleton. J Biol Chem 2009; 284: 27438-27448.

[12] DeAtley SM, Aksenov MY, Aksenova MV, Carney JM, Butterfield DA. Adriamycin induces protein oxidation in erythrocyte membranes. Pharmacol Toxicol 1998; 83: 62-68.

[13] Piwowar A, Knapik-Kordecka M, Warwas M. AOPP and its relations with selected markers of oxidative/antioxidative system in type 2 diabetes mellitus. Diabetes Res Clin Pract 2007; 77: 188-192.

[14] Witko-Sarsat V, Friedlander M, Capeillere-Blandin C, Nguyen-Khoa T, Nguyen AT, Zingraff J, Jungers P, Descamps-Latscha B. Advanced oxidation protein products as a novel marker of oxidative stress in uremia. Kidney Int 1996; 49: 1304-1313.

[15] Witko-Sarsat V, Friedlander M, Nguyen KT, Capeillere-Blandin C, Nguyen AT, Canteloup S, Dayer JM, Jungers P, Drüeke T, Descamps-Latscha B. Advanced oxidation protein products as novel mediators of inflammation and monocyte activation in chronic renal failure. J Immunol 1998; 161: 2524-2532.

[16] Zhou QG, Zhou M, Lou AJ, Xie D, Hou FF. Advanced oxidation protein products induce inflammatory response and insulin resistance in cultured adipocytes via induction of endoplasmic reticulum stress. Cell Physiol Biochem 2010; 26: 775-786.

[17] Wei XF, Zhou QG, Hou FF, Liu BY, Liang M. Advanced oxidation protein products induce mesangial cell perturbation through PKC-dependent activation of NADPH oxidase. Am J Physiol Renal Physiol 2009; 296: F427-F437.

[18] Zhou LL, Hou FF, Wang GB, Yang F, Xie D, Wang YP, Tian JW. Accumulation of advanced oxidation protein products induces podocyte apoptosis and deletion through NADPH-dependent mechanisms. Kidney Int 2009; 76: 1148-1160.

[19] Zhou QG, Peng X, Hu LL, Xie D, Zhou M, Hou FF. Advanced oxidation protein products inhibit differentiation and activate inflammation in 3T3-L1 preadipocytes. J Cell Physiol 2010; 225: 42-51.

[20] Guo ZJ, Hou FF, Liu SX, Tian JW, Zhang WR, Xie D, Zhou ZM, Liu ZQ, Zhang X. Picrorhiza scrophulariiflora improves accelerated atherosclerosis through inhibition of redox-sensitive inflammation. Int J Cardiol 2009; 136: 315-324.

[21] Baskol G, Demir H, Baskol M, Kilic E, Ates F, Karakukcu C, Ustdal M. Investigation of protein oxidation and lipid peroxidation in patients

with rheumatoid arthritis. Cell Biochem Funct 2006; 24: 307-311.
[22] Yang XB, Hou FF, Wu Q, Zhou H, Liu ZR, Yang Y, Zhang X. [Increased levels of advanced oxidation protein products are associated with atherosclerosis in chronic kidney disease]. Zhonghua Nei Ke Za Zhi 2005; 44: 342-346.
[23] Montagnani A, Gonnelli S, Alessandri M, Nuti R. Osteoporosis and risk of fracture in patients with diabetes: an update. Aging Clin Exp Res 2011; 23: 84-90.
[24] Sambrook PN. The skeleton in rheumatoid arthritis: common mechanisms for bone erosion and osteoporosis? J Rheumatol 2000; 27: 2541-2542.
[25] Stehman-Breen C. Osteoporosis and chronic kidney disease. Semin Nephrol 2004; 24: 78-81.
[26] Cunningham J, Sprague SM, Cannata-Andia J, Coco M, Cohen-Solal M, Fitzpatrick L, Goltzmann D, Lafage-Proust MH, Leonard M, Ott S, Rodriguez M, Stehman-Breen C, Stern P, Weisinger J; Osteoporosis Work Group. Osteoporosis in chronic kidney disease. Am J Kidney Dis 2004; 43: 566-571.
[27] Zhong ZM, Bai L, Chen JT. Advanced oxidation protein products inhibit proliferation and differentiation of rat osteoblast-like cells via NF-kappaB pathway. Cell Physiol Biochem 2009; 24: 105-114.
[28] Li HY, Hou FF, Zhang X, Chen PY, Liu SX, Feng JX, Liu ZQ, Shan YX, Wang GB, Zhou ZM, Tian JW, Xie D. Advanced oxidation protein products accelerate renal fibrosis in a remnant kidney model. J Am Soc Nephrol 2007; 18: 528-538.
[29] Kohler T, Beyeler M, Webster D, Muller R. Compartmental bone morphometry in the mouse femur: reproducibility and resolution dependence of microtomographic measurements. Calcif Tissue Int 2005; 77: 281-290.
[30] Sturmer EK, Seidlova-Wuttke D, Sehmisch S, Rack T, Wille J, Frosch KH, Wuttke W, Stürmer KM. Standardized bending and breaking test for the normal and osteoporotic metaphyseal tibias of the rat: effect of estradiol, testosterone, and raloxifene. J Bone Miner Res 2006; 21: 89-96.
[31] Alexander JM, Bab I, Fish S, Muller R, Uchiyama T, Gronowicz G, Nahounou M, Zhao Q, White DW, Chorev M, Gazit D, Rosenblatt M. Human parathyroid hormone 1-34 reverses bone loss in ovariectomized mice. J Bone Miner Res 2001; 16: 1665-1673.
[32] Waarsing JH, Day JS, Weinans H. An improved segmentation method for in vivo microCT imaging. J Bone Miner Res 2004; 19: 1640-1650.
[33] Bonnet N, Laroche N, Vico L, Dolleans E, Courteix D, Benhamou CL. Assessment of trabecular bone microarchitecture by two different x-ray microcomputed tomographs: a comparative study of the rat distal tibia using Skyscan and Scanco devices. Med Phys 2009; 36: 1286-1297.
[34] Chappard D, Retailleau-Gaborit N, Legrand E, Basle MF, Audran M. Comparison insight bone measurements by histomorphometry and microCT. J Bone Miner Res 2005; 20: 1177-1184.
[35] Akhter MP, Lappe JM, Davies KM, Recker RR. Transmenopausal changes in the trabecular bone structure. Bone 2007; 41: 111-116.
[36] Bouxsein ML, Boyd SK, Christiansen BA, Guldberg RE, Jepsen KJ, Müller R. Guidelines for assessment of bone microstructure in rodents using micro-computed tomography. J Bone Miner Res 2010; 25: 1468-1486.
[37] Akesson K, Ljunghall S, Jonsson B, Sernbo I, Johnell O, Gärdsell P, Obrant KJ. Assessment of biochemical markers of bone metabolism in relation to the occurrence of fracture: a retrospective and prospective population-based study of women. J Bone Miner Res 1995; 10: 1823-1829.
[38] Valimaki MJ, Farrerons-Minguella J, Halse J, Kroger H, Maroni M, Mulder H, Muñoz-Torres M, Sääf M, Snorre Øfjord E. Effects of risedronate 5 mg/d on bone mineral density and bone turnover markers in late-postmenopausal women with osteopenia: a multinational, 24-month, randomized, double-blind, placebo-controlled, parallel-group, phase III trial. Clin Ther 2007; 29: 1937-1949.
[39] Calvo MS, Eyre DR, Gundberg CM. Molecular basis and clinical application of biological markers of bone turnover. Endocr Rev 1996; 17: 333-368.
[40] Rosen HN, Moses AC, Garber J, Iloputaife ID, Ross DS, Lee SL, Greenspan SL. Serum CTX: a new marker of bone resorption that shows treatment effect more often than other markers because of low coefficient of variability and large changes with bisphosphonate therapy. Calcif Tissue Int 2000; 66: 100-103.
[41] Lerner UH. Bone remodeling in post-menopausal osteoporosis. J Dent Res 2006; 85: 584-595.
[42] Keller JN, Kindy MS, Holtsberg FW, St CD, Yen HC, Germeyer A, Steiner SM, Bruce-Keller AJ, Hutchins JB, Mattson MP. Mitochondrial manganese superoxide dismutase prevents neural apoptosis and reduces ischemic brain injury: suppression of peroxynitrite production, lipid peroxidation, and mitochondrial dysfunction. J Neurosci 1998; 18: 687-697.
[43] Linnane AW, Eastwood H. Cellular redox regulation and prooxidant signaling systems: a new

perspective on the free radical theory of aging. Ann N Y Acad Sci 2006; 1067: 47-55.
[44] Sendur OF, Turan Y, Tastaban E, Serter M. Antioxidant status in patients with osteoporosis: a controlled study. Joint Bone Spine 2009; 76: 514-518.
[45] Fraser JH, Helfrich MH, Wallace HM, Ralston SH. Hydrogen peroxide, but not superoxide, stimulates bone resorption in mouse calvariae. Bone 1996; 19: 223-226.
[46] Suda N, Morita I, Kuroda T, Murota S. Participation of oxidative stress in the process of osteoclast differentiation. Biochim Biophys Acta 1993; 1157: 318-323.